

## NUMERICAL ANALYSIS OF RESIDUAL STRESS DISTRIBUTION IN RIVETED LAP JOINT UNDER TENSION

Wojciech Wronicz

*Institute of Aviation*  
Krakowska Av. 110/114, 02-256 Warsaw, Poland  
tel.: +48 22 1883688, fax: +48 22 8685680  
e-mail: wojciech.wronicz@ilot.edu.pl

### Abstract

*Riveted joints are a common location of fatigue cracks in aircraft metal structures. Fatigue life of such joints as well as a place of cracks nucleation is strongly influence by a stress distribution in sheets, which is a result of residual stresses (mainly after riveting) and stresses induced by external loads. Stress distribution in two-row lap joint was investigated with the use of Finite Element Method. The joint consist of two 1.5 mm sheets and two protruding rivets with diameter equal to 4 mm, made of 2024 T3 (sheets) and 2117 T4 (rivets) aluminium alloys. The simulations covered a riveting process and tensile stages. The 3D models of joint with the universal rivets and with the brazier, rivets with a compensator were prepared. Elastoplastic material properties as well as geometric nonlinearity and contact phenomena were included. The results of simulations show that the residual stress distribution after release of tensile loading varies significantly from the distribution after riveting only. This fact should therefore be taken into account in a fatigue life estimation of such joints performed based on a FE calculation. The paper presents also the influence of the analysed rivet geometry on the stress distribution at the sheets faying surfaces.*

**Keywords:** joint, rivet, fatigue, residual stress, finite element

### 1. Introduction

Fatigue properties are extremely important in airframe design since they influence directly aircraft service life and its maintenance costs (inspections and repairs). Moreover, fatigue is the main source of failure in aircraft [2, 12]. The most popular type of aircraft structure is still a metal semi-monocoque with elements (skins, stringers, ribs and frames) jointed with rivets. Riveted joints are a common location of fatigue cracks. At the same time, fatigue life of such joints as well as a place of cracks nucleation is strongly influenced by riveting technology. A riveting force level alone can change the fatigue life of the same specimens more than ten times [5, 6]. This effect is caused mainly by a stress distribution around rivets [5, 7, 15]. Riveting geometry is a factor, which has an effect on the residual stress system [14]. From the fatigue point of view, compressive stresses are beneficial since they delay crack initiation and growth.

The stress system around rivets is a result of residual stresses after manufacturing (mainly riveting) and stresses induced by external loads. After riveting radial stresses around a rivet are compressive. Tangential stresses are tensile in the case of low riveting force. For high squeezing force, near a rivet tangential stresses are compressive [5, 15]. This residual stress system is modified during joint loading.

Typical type of a riveted joint, especially in an aircraft fuselage design, is a lap joint. Stress distribution in such joint during tension was investigated by various researchers [1, 3, 8, 11]. They analyse tangential stresses, as well as contact stresses between sheets and fretting damages around holes. In the case of a numerical calculations, simulations focus usually on a state after riveting and during tension loading.

The aim of the presented study is to analyse a stress progress in two-row lap joint during riveting, loading as well as unloading with the use of Finite Element Method. Influence of

a rivet geometry, namely existence of a compensator, is investigated also. Results from the vicinity of the top-row rivet (rivet no. 1 in Fig. 3) at the mating surface of the outer sheet are presented only due to restricted scope of this paper and since this is an area where fatigue cracks usually nucleate in similar riveted lap joints [3, 8]. This location is practically inaccessible for experimental methods.

## 2. Analysed joint

The study concerns two-row lap joints with geometry presented in Fig. 1. The joint consists of two 1.5 mm sheets and two protruding rivets with diameter equal to 4 mm, made of the 2024 T3 (sheets) and the 2117 T4 (rivets) aluminium alloys. One column of rivets (area marked with a blue dashed line in Fig. 1) was analysed. The symmetry conditions on the cutting-planes between rivets columns (pink centre line) were assumed during the loading stage due to interactions of not-modelled part of the joint (analogically to the plane-strain conditions).

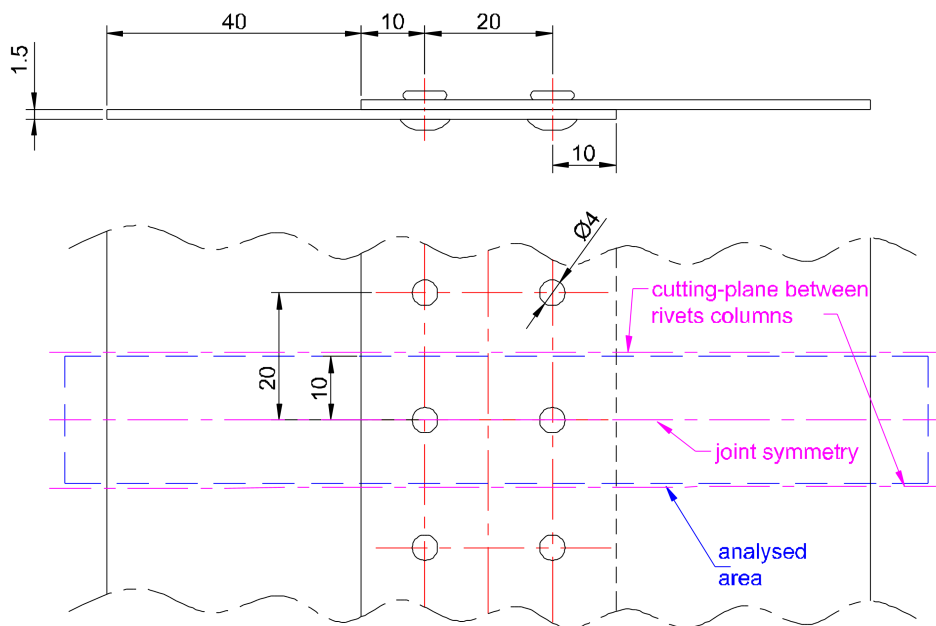


Fig. 1. Geometry of analysed joint

Two types of rivet geometry were analysed, namely the universal rivet according to the MS20470 standard and the brazier rivet with a compensator according to the Russian standard OST 1 34040-79 (Fig. 2). The compensator is a small protruding part of the manufactured head, which is pushed into the head during riveting. The 2117 T4 alloy was used for both rivet types despite that the standard OST 1 34040-79 designates the Polish PA25 aluminium alloy. The aim of this investigation was to study an influence of a rivet geometry. Moreover, observations presented in [10] indicate that the 2117 T4 alloy is more appropriate for this type of rivet.

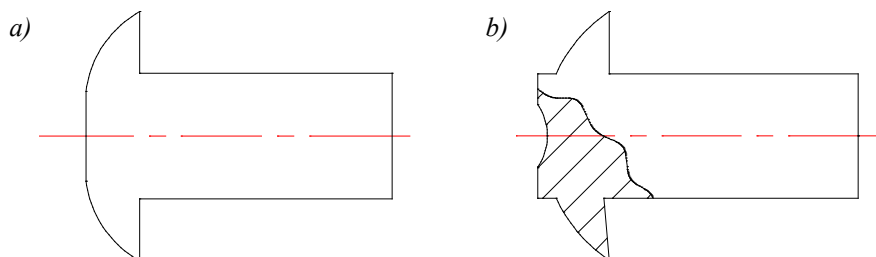


Fig. 2. Rivets geometry: a) universal rivet MS20470, b) rivet with compensator OST 1 34040-79

### 3. Model

The 3D models of the joint with assumed rivet geometries for the FE analyses were prepared. Because of the symmetry, only a half of the analysed area was represented and the symmetry conditions were set for all nodes in the joint symmetry plane. The simulation consists of riveting and loading stages. Because rivets usually are not squeezed simultaneously in all column, the symmetric conditions on the cutting-plane between rivet columns are not true. It was taken into account by introducing additional sheets, which are numerically glued to the internal and external sheets. Each model contains about 130 000 linear elements and 150 000 nodes. The 8-node (brick) and some amount of 6-node (wedges) solid elements were used. Except the additional sheets, each model consist of four deformable (two rivets and two sheets) and five rigid (two hold-ones, two press stamps and surface which introduce loading) bodies. The model was shown in Fig. 3.

During the riveting, both hold-ones are fixed and punches can move only in the vertical direction (z). Moreover, displacements in the tension direction (x) of nodes on the sheets outer ends were restricted. The sheets are clamped together by forces applied to the nodes on the internal sheet surface near the rivets. Then, forces are applied to the punches and increase to its maximum. After that, all forces are released. The force value of 25 kN per rivet (12.5 kN per half of a rivet in the model) was adjusted experimentally to obtain a driven head diameter 1.7 times higher than a rivet shank diameter.

After riveting, the additional sheets were deactivated and the symmetry conditions were set on the cutting-plane between rivets columns. Nodes on the outer end of the external sheet (left in Fig. 3) were fixed. Nodes on the outer end of the internal sheet (right in Fig. 3) can move only in the tension direction (x). The joint was loaded by tension force applied to the rigid surface glued to the outer end of the internal sheet (right in Fig. 3). The force increase to 1.5 kN (100 MPa in a sheet outside the joint) and then is released.

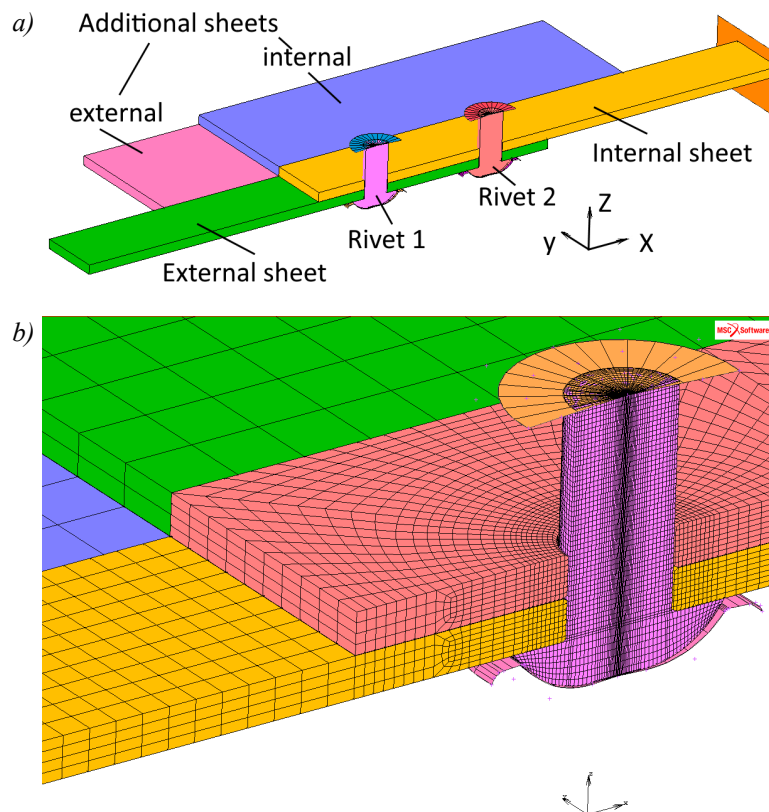


Fig. 3. FE model: a) overall view, b) mesh near rivet no. 1

Material elastoplastic behaviour as well as geometrical nonlinearity and contact phenomena were taken into account with the use of MSC MARC nonlinear implicit algorithm. The models of the 2024 T3 alloy (sheets) and the 2117 T4 alloy (rivets) used in previous analyses [13, 15, 16] were selected. Fig. 4 presents stress-strain curves of the used material models. The stick-slip friction model [4] was used for contact interactions. The friction coefficient equal to 0.34 for kinematic and 0.42 for static contact were selected for aluminum – aluminum pairs (sheets and rivet). For aluminum – steel (tools) pairs these coefficient were equal to 0.15 and 0.186 respectively. Values of coefficient were selected based on [17].

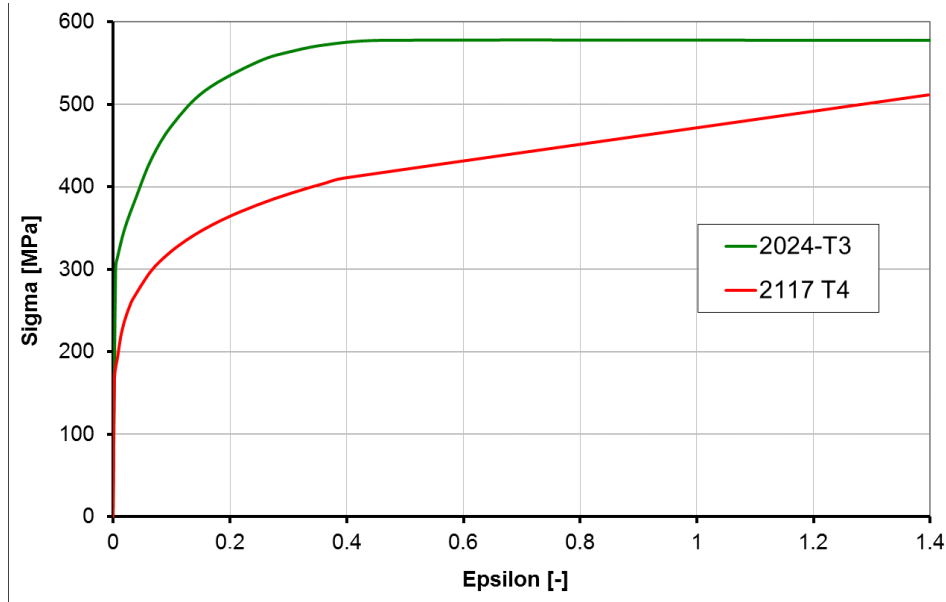


Fig. 4. Material models

#### 4. Model verification

The model with the universal rivet was verified by comparison of the force-displacement curves of the press punch recorded during riveting on a testing machine and obtained in numerical simulation. In the experiment, the displacements were measured by a testing machine sensor and include a flexibility of the machine elements. In order to consider this, displacements caused by this flexibility were measured during squeezing of a small piece of steel and then subtracted from the displacements recorded during riveting. Quite good correlation of numerical and experimental data was obtained (Fig. 5). In the case of a comparison between strains recorded by strain gauges near a driven head and obtained in calculations, such a good correspondence was not obtained and therefore this analysis is rather qualitative than quantitative. This inconsistency of numerical and experimental results can arise from some differences in material properties and test details. However, the aim of this study is not to determine stresses in a particular joint but to investigate a stress progress in this type of joints and the influence of the rivet geometry. The verification of the model with the rivet with a compensator was not conducted since this type of rivet is available made of the PA25 alloy only.

#### 5. Results

Figure 6 and 7 present tangential and radial stresses at the mating surface of the outer sheet, along the path in the net section of the top-row rivet (rivet no. 1 in Fig. 3) for both rivet types. The path is transverse to the tension direction and was marked in the figure on the graph. In the case of the universal rivet, results for the 0.98% of maximum tension loading are presented since the data for the maximum loading unfortunately were not recorded.

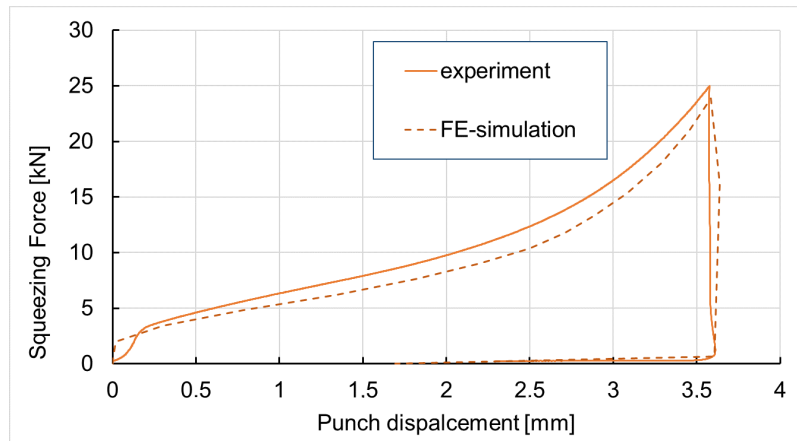


Fig. 5. Force-displacement curve of press punch

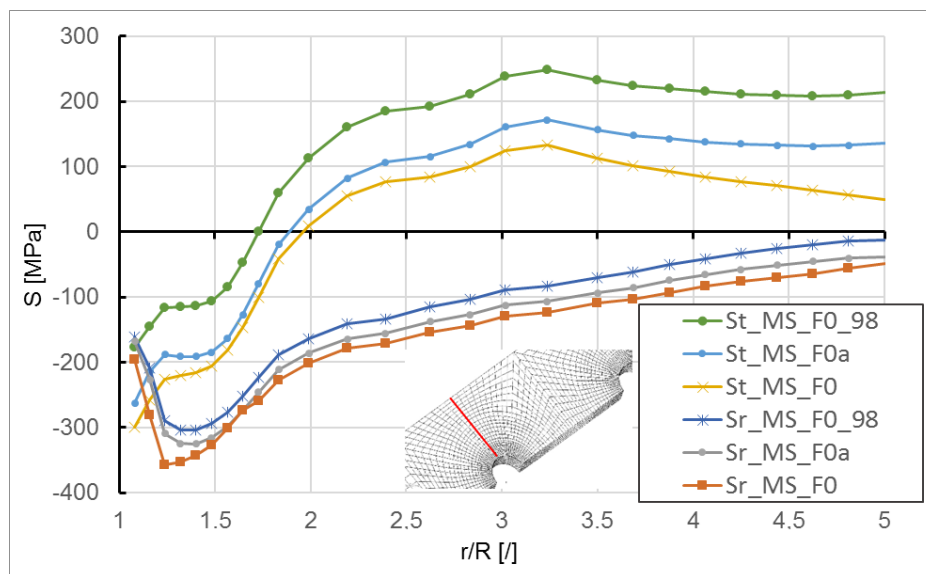


Fig. 6. Stresses along marked path,  $St$ ,  $Sr$  – tangential and radial stresses,  $MS$  – universal rivet,  $F0$  – after riveting,  $F0_{98}$  – 98% of maximum tension,  $F0a$  – after unloading,  $r$  – distance from rivet axis,  $R$  – rivet radius

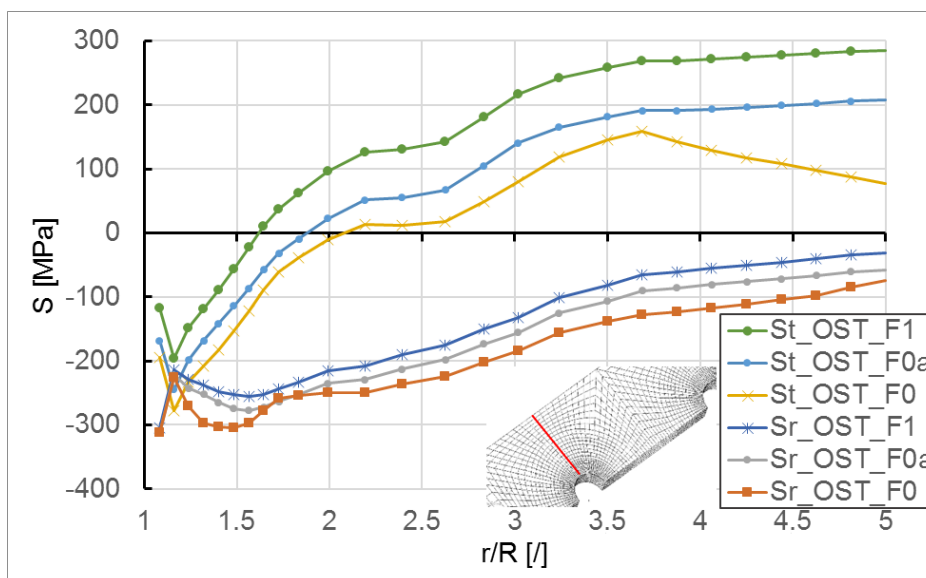


Fig. 7. Stresses along marked path,  $St$ ,  $Sr$  – tangential and radial stresses,  $OST$  – rivet with compensator,  $F0$  – after riveting,  $F1$  – maximum tension,  $F0a$  – after unloading,  $r$  – distance from rivet axis,  $R$  – rivet radius

Residual tangential stresses which were induced during riveting (F0), during tension loading increase significantly to its maximum (F0\_98 and F1) and then decrease during unloading (F0a). There is a substantial difference between the stress distribution after riveting only and after unloading. These differences are minor near the rivet and increase with a distance from the rivet axis. In the case of the universal rivet (Fig. 6), the maximum tangential stresses occur for the relative radial position  $r/R$  equal to 3.2. Above this value the slope of the stress curves is lower, after the joint loading (F0\_98 and F0a) than after riveting (F0).

The stress distribution for the rivet with a compensator (Fig. 7) is similar, but the maximum of tangential stresses after riveting (F0) is further from the rivet ( $r/R = 3.7$ ). Moreover, during tension this maximum shifts to the plane between rivet columns ( $r/R = 5$ ).

Stress distribution of the radial stresses did not change significantly during tension and unloading since these stresses on the chosen path are perpendicular to the direction of a tension.

During a constant amplitude fatigue test (with tensile loads only), the stresses varies between distribution for the maximum and minimum loads (unloading). The difference between maximum and minimum stresses is an amplitude. Fig. 8 presents stress distribution in these loading cases for the analysed rivets.

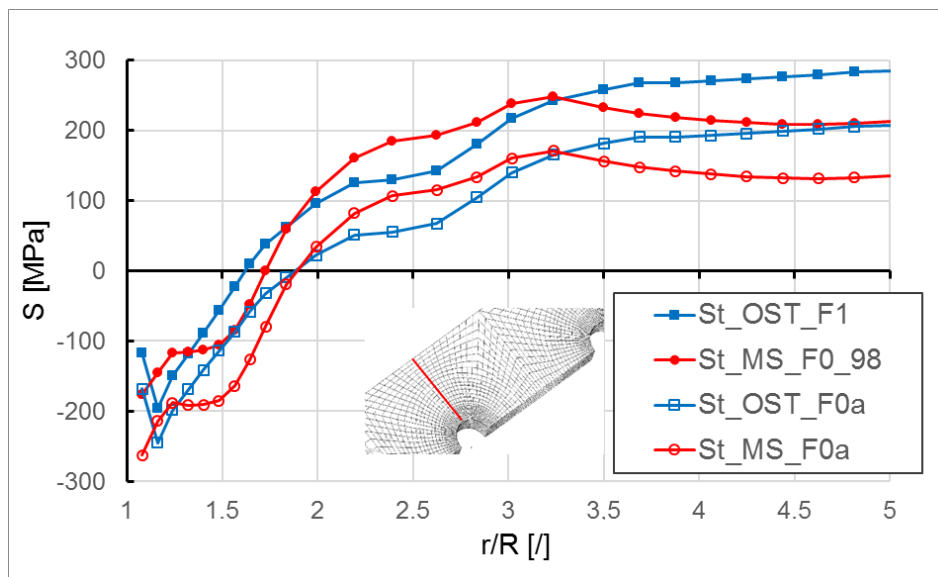


Fig. 8. Stresses along marked path,  $St$  – tangential stresses,  $MS$  – universal rivet,  $OST$  – rivet with compensator,  $F0_{98}$  – 98% of maximum tension,  $F1$  – maximum tension,  $F0a$  – after unloading,  $r$  – distance from rivet axis,  $R$  – rivet radius

The differences between stresses during maximum and minimum loads (amplitudes) are similar for both models. Very near the rivet hole, the tangential stresses are at the same level. For the  $r/R$  parameter between about 1.3 and 1.8, the stress curves for the universal rivet are under curves for the rivet with a compensator. This is an area, where tangential stresses are mainly compressive. Above this value of the  $r/R$  parameter, stresses became tensile for both types and are higher in the case of the universal rivet. At the distance from rivet axis equal to about 3.2 rivet radius, the tangential stresses for the universal rivet reach their maximums and also became lower than stresses for the rivet with a compensator. In the last part of the graph, the tangential stresses for the rivet with a compensator are increasing. They are higher than stresses for the universal rivet, which are decreasing.

In the case of a low riveting force, fatigue cracks in lap joints usually nucleates at a hole edge, which is a notch and causes a stress concentration. When the squeezing force is higher, compressive residual stresses prevent crack nucleation at a hole edge and cracks originate usually

in a small distance from this location, in the area of heavy fretting damage, at the edge of contact between sheets [1, 8]. In Fig. 8, this is a distance range where compressive tangential stresses are higher for the universal rivet. Further increase of the riveting force causes that a majority of load is transfer through a friction between sheets, instead of bearing stresses between the rivet and sheets. As a result, cracks start much further and growth outside the hole [9]. At this location, tangential stresses in Fig. 8 are tensile and are lower for the rivet with a compensator. However, it should be noted, that higher squeezing force caused also, that crack origin move from the sheet net section [5, 8, 9], what was not included in this analysis.

From the fatigue point of view, the universal rivet offers a more beneficial stress distribution in the close vicinity of the rivet hole, where these stresses are compressive. In the area where tangential stresses are tensile and there are contact stresses between sheets (clamping), more advantageous situation is in the case of the rivet with a compensator. Compressive stresses restrict possibility of crack nucleation, what indicate a better fatigue characteristic of the rivet with a compensator. This type of the rivet presented a longer fatigue life in comparison with the universal rivet in tests reported in [10]. However, this fatigue tests concern three-row joints, relative diameter of a driven head was lower ( $D/D_o = 1.5$ ) and there are also some differences in rivets and sheet dimensions.

## 6. Conclusions

Stress distribution in a critical area of the lap joint was analysed with the use of the Finite Element Method. The results of simulations show that the residual stress distribution after release of tensile loading varies significantly from the distribution after riveting only. This fact should therefore be taken into account in a fatigue life estimation of such joints performed based on FE calculations.

From the fatigue point of view, the universal rivet offers a more beneficial stress distribution in the close vicinity of the rivet hole, where these stresses are compressive. Further from the rivet hole, where tangential stresses are tensile, more advantageous situation is in the case of the rivet with a compensator. Since compressive stresses restrict possibility of crack nucleation, better fatigue characteristic could be expected from the rivet with a compensator.

The rivet with a compensator has been design for another alloy and lower relative driven head diameter ( $D/D_o$ ). Probably it is possible to improve its fatigue performance by optimisation of a compensator geometry for analysed conditions.

## References

- [1] Brown, A. M., Straznicky, P. V., *Simulating fretting contact in single lap splices*, Int. J. Fatigue, Vol. 31, No. 2, pp. 375-384, 2009.
- [2] Findlay, S. J., Harrison, N. D., *Why aircraft fail*, Mater. Today, Vol. 5, No. 11, pp. 18-25, 2002.
- [3] Li, G., et al., *Stress in triple-row riveted lap joints under the influence of specific factors*, J. Aircr., Vol. 48, No. 2, pp. 527-539, 2011.
- [4] *Marc 2014.1 Theory and user information*, Vol. A, MSC Software Corporation, USA 2014.
- [5] Müller, R. P. G., *An experimental and analytical investigation on the fatigue behaviour of fuselage riveted lap joints*, Delft University of Technology, Delft 1995.
- [6] Müller, R. P. G., Hart-Smith, L. J., *Making fuselage riveted lap splices with 200-year crack-free-lives*, Proceedings of 19th ICAF Symposium, Fatigue in New and Aging Aircraft, pp. 18-20, Edinburgh 1997.
- [7] Rans, C., et al., *Riveting process induced residual stresses around solid rivets in mechanical joints*, J. Aircr., Vol. 44, No. 1, pp. 323-329, 2007.
- [8] Rans, C. D., *The role of rivet installation on the fatigue performance of riveted lap joints*,

- Carleton University, Carleton 2007.
- [9] Skorupa, A., Skorupa, M., *Riveted lap joints in aircraft fuselage: design, analysis and properties*, Springer, Dordrecht, New York 2012.
- [10] Skorupa, M., et al., *Effect of production variables on the fatigue behaviour of riveted lap joints*, Int. J. Fatigue, Vol. 32, No. 7, pp. 996-1003, 2010.
- [11] Szymczyk, E., *Numeryczna analiza zjawisk lokalnych w połączeniach nitowych konstrukcji lotniczych*, Military University of Technology, Warsaw 2013.
- [12] Tavares, S. M. O., de Castro, P. M. S. T., *An overview of fatigue in aircraft structures*, Fatigue Fract. Eng. Mater. Struct., Vol. 40, No. 10, pp. 1510-1529, 2017.
- [13] Wronicz, W., *Comparison of residual stress state on sheets faying surface after standard and NACA riveting-numerical approach*, Fatigue Aircr. Struct., Vol. 2016, No. 8, pp. 116-126, Warsaw 2016.
- [14] Wronicz, W., et al., *Experimental and numerical study of stress and strain field around the rivet*, ICAF 2011 Structural Integrity: Influence of Efficiency and Green Imperatives, Komorowski, J., (ed.), pp. 277-288, Dordrecht 2011.
- [15] Wronicz, W., Kaniowski, J., *Experimental and numerical study of strain progress during and after riveting process for brazier rivet and rivet with compensator – squeezing force and rivet type effect*, Fatigue Aircr. Struct., Vol. 2011, No. 3, pp. 166-190, Warsaw 2011.
- [16] Wronicz, W., Kaniowski, J., *The analysis of the influence of riveting parameters specified in selected riveting instructions on residual stresses*, Fatigue Aircr. Struct., Vol. 2014, No. 6, pp. 63-71, Warsaw 2015.
- [17] ASM International, Materials Park, *Friction, lubrication, and wear technology*, ASM Handbook, Vol. 18, Ohio 1992.

*Manuscript received 27 July 2018; approved for printing 29 October 2018*